

# Adipose tissue mass is modulated by *SLUG* (*SNAI2*)

Pedro Antonio Pérez-Mancera<sup>1</sup>, Camino Bermejo-Rodríguez<sup>1</sup>, Inés González-Herrero<sup>1</sup>, Michel Herranz<sup>1</sup>, Teresa Flores<sup>2</sup>, Rafael Jiménez<sup>3</sup> and Isidro Sánchez-García<sup>1,\*</sup>

<sup>1</sup>Experimental Therapeutics and Translational Oncology Program, Instituto de Biología Molecular y Celular del Cáncer (IBMCC), CSIC, <sup>2</sup>Servicio de Anatomía Patológica and <sup>3</sup>Departamento de Fisiología y Farmacología, Universidad de Salamanca, Campus M. Unamuno, 37007 Salamanca, Spain

Received July 13, 2007; Revised September 5, 2007; Accepted September 19, 2007

The zinc-finger transcription factor *SLUG* (*SNAI2*) triggers epithelial–mesenchymal transitions (EMTs) and plays an important role in the developmental processes. Here, we show that *SLUG* is expressed in white adipose tissue (WAT) in humans and its expression is tightly controlled during adipocyte differentiation. *Slug*-deficient mice exhibit a marked deficiency in WAT size, and *Slug*-overexpressing mice (Combi-*Slug*) exhibit an increase in the WAT size. Consistent with *in vivo* data, *Slug*-deficient mouse embryonic fibroblasts (MEFs) showed a dramatically reduced capacity for adipogenesis *in vitro* and there was extensive lipid accumulation in Combi-*Slug* MEFs. The analysis of adipogenic gene expression both *in vivo* and *in vitro* showed that peroxisome proliferator-activated factor  $\gamma$ 2 (PPAR $\gamma$ 2) expression was altered. Complementation studies rescued this phenotype, indicating that WAT alterations induced by *Slug* are reversible. Our results further show a differential histone deacetylase recruitment to the PPAR $\gamma$ 2 promoter in a tissue- and *Slug*-dependent manner. Our results connect, for the first time, adipogenesis with the requirement of a critical level of an EMT regulator in mammals. This work may lead to the development of targeted drugs for the treatment of patients with obesity and/or lipodystrophy.

## INTRODUCTION

Being overweight or obese increases the risk of many diseases and health conditions. Therefore, a better knowledge of the molecular mechanisms that control adipose tissue development and function is an important goal for understanding the causes, prevention and treatment of obesity. Previous studies have identified a number of transcription factors involved in adipocyte differentiation. These include peroxisome proliferator-activated factor  $\gamma$  (PPAR $\gamma$ ) and members of the C/EBP family of transcription factors (1,2). Although many of the components of the gene regulatory network that controls the differentiation of adipocytes have been elucidated in studies of cultured 3T3-L1 pre-adipocytes and primary mouse embryonic fibroblasts (MEFs), recent evidence has suggested that additional factors are likely to be necessary *in vivo* (3,4).

The zinc-finger transcription factor *SLUG* (*SNAI2*) is a member of the Snail family of zinc-finger transcription factors that share an evolutionary conserved role in mesoderm formation in invertebrates and vertebrates. *SLUG* is an important regulator of normal and tumour development (5,6). *Slug* controls key aspects of stem cell function, suggesting that similar mechanisms

control normal development and cancer stem cell properties (7–10). The post-natal expression of *SLUG* (*SNAI2*) and the effects of *SLUG* deletion and overexpression are similar in mouse and human (8,10–15). Homozygous-null *Slug* mice have a white forehead blaze, patchy depigmentation of the ventral body, tail and feet and macrocytic anaemia and infertility, inferring an essential role for *Slug* in melanocytes, haematopoietic stem cells and germ cells (8). Heterozygous deletion of the *SNAI2* gene results in human piebaldism (14), whereas a homozygous deletion has been detected in two individuals with Waardenburg disease type 2 (12). Recent studies showed that *Slug* is tightly controlled temporally and spatially in a number of sites including the neural crest and haematopoietic system (7,8). Regarding the major adult tissues, transcripts of the *Slug* gene are present in white adipose tissue (WAT) in mice (10), suggesting a potential role for *Slug* in adipogenesis. However, the functions of *SLUG* in adipocyte development *in vivo* and *in vitro* remain unknown.

In this study, we found that *SLUG* is expressed in human WAT tissue. *Slug* expression is tightly controlled during adipocyte differentiation in both 3T3-L1 and primary murine

\*To whom correspondence should be addressed. Tel: +34 923238403; Fax: +34 923294813; Email: isg@usal.es

embryonic fibroblast (MEFs), suggesting that Slug is also required for adipogenesis. Slug-deficient mice carried much less WAT mass than wild-type mice, showing Slug also plays a role in WAT development *in vivo*. In agreement with these results, mice carrying a tetracycline-repressible Slug transgene (Combi-Slug) exhibit an increase in the WAT mass, and this increase in the WAT tissue was restored by suppression of the *Slug* transgene. Thus, it seems likely that failure to regulate Slug expression explains why Combi-Slug mice develop obesity. Consistent with *in vivo* data, Slug-deficient MEFs showed a dramatically reduced capacity for adipogenesis *in vitro* when compared with wild-type MEFs. However, there was extensive lipid accumulation in Combi-Slug MEFs. We therefore analysed the molecular mechanism by which Slug controls WAT development and found that PPAR $\gamma$ 2 expression is altered both *in vivo* in WAT of Slug-deficient and Combi-Slug mice and *in vitro* in Slug-deficient and Combi-Slug MEFs during the course of adipocytic differentiation. Complementation studies in Slug-deficient MEFs confirmed this regulation. Histone acetylation status is related to Slug expression in adipose tissue, and chromatin immunoprecipitation (ChIP) assays show differential histone deacetylase (HDAC) recruitment to the PPAR $\gamma$ 2 promoter in a tissue- and Slug-dependent manner. These results provide evidence that Slug is a key regulator of the adipocyte differentiation both *in vivo* and *in vitro* and indicate that loss of tight control of Slug expression can induce obesity and/or lipodystrophy in mice. Because Slug is also expressed in human white fat, this work may lead to the development of targeted drugs for the treatment of these pathologies in humans.

## RESULTS

### SLUG is expressed in white fat in humans

*SLUG* (*SNAI2*) expression and the effects of its deletion and overexpression are similar in mouse and human (8,10–15). Our previous observations indicated that Slug was also present in mouse adipose tissue (10 and Fig. 1A–E). Thus, now we first studied whether human adipose tissue expressed *SLUG*. Expression of human *SLUG* was analysed by reverse transcriptase–polymerase chain reaction (RT–PCR). The PCR products were transferred to a nylon membrane and analysed by hybridization with a specific probe. *SLUG* expression was identified in human subcutaneous adipose tissues (Fig. 1B and C). These and previous observations (10) indicate that expression of *SLUG* is a common finding in both human and mouse WAT, suggesting a role for *SLUG* in WAT development.

### Slug expression is tightly controlled during adipocyte differentiation

To determine the function of Slug in WAT development, we first examined expression of Slug during adipocyte differentiation. 3T3-L1 pre-adipocytes are a well-characterized *in vitro* model of adipocyte differentiation that can differentiate into mature adipocytes upon exposure to a mixture hormonal stimulus (2–4). Slug expression is very high before induction of differentiation and the amount of Slug mRNA and protein decreased during such hormonal stimulation (Fig. 2A and B),

whereas PPAR $\gamma$ , a transcription factor essential for adipocyte differentiation (2), was apparent within 1 day and increased in abundance thereafter (Fig. 2B). This observation was further confirmed using primary MEFs as a model (Fig. 2C). These results indicate that Slug is tightly controlled temporally during differentiation of pre-adipocytes.

### Slug-deficient mice exhibit reduced WAT mass

In order to determine the effect of Slug expression in WAT development, we analysed WAT mass in Slug-deficient mice. We observed modest but significant reduction of body weight in Slug-deficient mice (Supplementary Material, Fig. S1). Slug-deficient mice showed a large reduction in WAT weight in Slug  $-/-$  mice (Table 1 and Fig. 3), but heterozygous mice were indistinguishable from wild-type mice (data not shown). As control for decreased fat mass, we compared the muscle tissue of control and Slug  $-/-$  mice and we did not find any difference. However, Slug-deficient animals were protected against obesity induced by a high-fat diet (16) (Supplementary Material, Fig. S1). In addition, food intake was similar in wild-type ( $2.9 \pm 0.4$  g per mouse per day) and Slug-deficient mice ( $3.0 \pm 0.4$  g per mouse per day). In the animals fed the high-fat diet, fat pads in Slug-deficient mice showed no significant changes, but these pads had showed dramatic increases in the wild-type littermates, leading to an even more dramatic difference (data not shown). This overall reduction in adipose tissue in Slug-deficient mice was observed in males and females (Table 1). In contrast to WAT, other tissues including kidney (Table 1) and the interscapular brown adipose tissue (BAT) and liver (data not shown) had similar weights for wild-type and Slug-deficient mice.

To further characterize the phenotype of adipose tissue, we examined histological sections of WAT and BAT (Figs 3 and 4). We observed no difference between the wild-type and KO mice in the BAT and WAT tissues. The histological analyses of the WAT in Slug-deficient mice did not evidence any pathological change within the terminally differentiated adipocytes. On the contrary, Slug-deficient mice had a normal architecture of the tissue and we did not observe any shift in the WAT towards immature tissue in the Slug-deficient mice.

To confirm that the decrease in the WAT mass in Slug-deficient mice was caused by the absence of Slug, Slug-deficient mice were crossed with Combi-Slug mice (10), which express the transgenic Slug in WAT tissue (Fig. 1A). As expected, the WAT phenotype was rescued in the Slug-deficient mice by expressing Slug (Table 1).

We also investigated whether increased energy expenditure could account for the decrease in WAT mass in Slug-deficient mice by studying core body temperature and locomotor activity in these mice. We have measured locomotor activity and body temperature in Slug-deficient mice (Supplementary Material, Table S1), showing no significant differences.

### Slug expression modulates WAT mass in mice

The above results suggest that Slug controls WAT tissue mass. Thus, we next evaluated the effect of upregulation of *Slug* expression on WAT mass *in vivo*. Mice carrying a

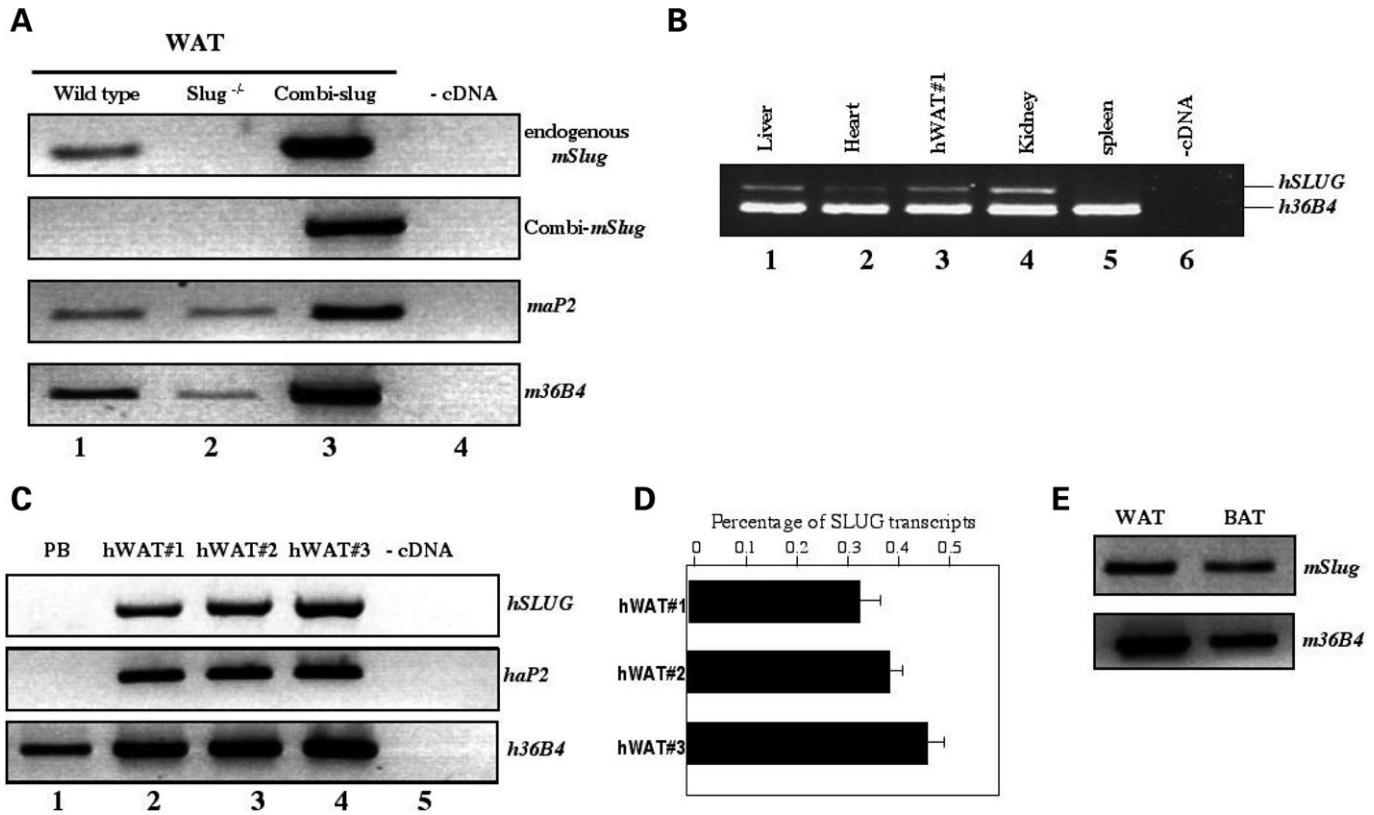


**Figure 1.** SLUG expression in WAT. Expression of both human and mouse *Slug* was analysed by RT-PCR. 36B4 were used to check cDNA integrity and loading. (A) *Slug* expression in mouse WAT. Expression of Combi-Slug, endogenous *Slug* and adipocyte fatty acid-binding protein (aP2) was analysed by RT-PCR in WAT derived of Combi-Slug, *Slug*-deficient mice and control mice. The PCR products were transferred to a nylon membrane and analysed by hybridization with a specific probe. (B) *SLUG* expression in human tissues. Expression of endogenous *SLUG* was analysed by RT-PCR in a variety of human tissues like liver (1), heart (2), hWAT#1 (3), kidney (4), spleen (5) and no cDNA (6). (C) *SLUG* expression in human adipose tissue. Expression of endogenous *SLUG* and adipocyte fatty acid-binding protein (aP2) was analysed by RT-PCR in human subcutaneous adipose tissue RNA (Zen-bio, Inc.) corresponding to donors with different BMI. Human peripheral blood as a tissue where human *SLUG* is not expressed (lane 1), human subcutaneous adipose tissue coming from a donor with a BMI=21.23 (hWAT#1, lane 2), human subcutaneous adipose tissue coming from a donor with a BMI=27.37 (hWAT#2, lane 3), human subcutaneous adipose tissue coming from a donor with a BMI=32.55 (hWAT#3, lane 4) and no cDNA (lane 5). (D) Quantification of *SLUG* (*SNAI2*) expression by real-time PCR in human adipose tissues. Percentage of *SLUG* transcripts with reference to  $\beta$ -actin is shown in hWAT#1, hWAT#2 and hWAT#3 human adipose tissue samples. Values are mean  $\pm$  SEM of three independent experiments. Differences between hWAT#1 and hWAT#3 were statistically significant ( $P < 0.05$ ) as determined by Mann-Whitney's test. However, each hWAT sample comes from only one individual and the apparent correlation between the BMI and *SLUG* expression may depend on population variation. (E) *Slug* expression in BAT. Expression of mouse *Slug* was analysed by RT-PCR in BAT derived of control mice.

tetracycline-repressible *Slug* transgene (Combi-Slug mice) were initially generated to investigate the potential role of *SLUG* overexpression in cancer (10). As anticipated from the patterns of *Slug* expression, Combi-Slug mice expressed high amounts of *Slug* in adipose tissue (10; Fig. 1A). We now analysed WAT in *Slug*-overexpressing mice. Transgenic mice kept off doxycycline from conception, leading to *Slug* expression throughout development, were found to have a modest but significant increase in body weight (Supplementary Material, Fig. S1) and to have strikingly increased WAT mass. Uniformly, male and female *Slug*-overexpressing mice show a significant increase in the WAT weight (Table 1 and Fig. 3), indicating that the overexpression of *Slug* does perturb normal WAT mass. Moreover, food intake in Combi-Slug mice ( $2.9 \pm 0.6$  g per mouse per day) was similar to wild-type mice.

We also investigated whether decreased energy expenditure could account for the increase in WAT mass in *Slug*-Combi

mice by studying core body temperature and locomotor activity in these mice. We have measured locomotor activity and body temperature in Combi-Slug mice (Supplementary Material, Table S1), showing no significant differences.

Some Combi-Slug animals (12%) presented lipid accumulation in kidney and liver (Fig. 5A) and developed palpable masses involving the adipose tissues, which upon dissection and histological examination revealed lipoma formation (Fig. 5B). Similarly to *Slug*-deficient mice, the histological analyses of the white adipose depots in the *Slug*-overexpressing animals revealed a normal architecture of the tissue (Fig. 3). However, the volumes of adipocytes of Combi-Slug mice were larger than those of normal mice (Fig. 3C). Pathological changes were not observed in the BAT of these transgenic mice (Fig. 4). Thus, *Slug*-overexpressing mice exhibit increased WAT mass. This result is in agreement with the loss of the physiological modulation of *Slug*

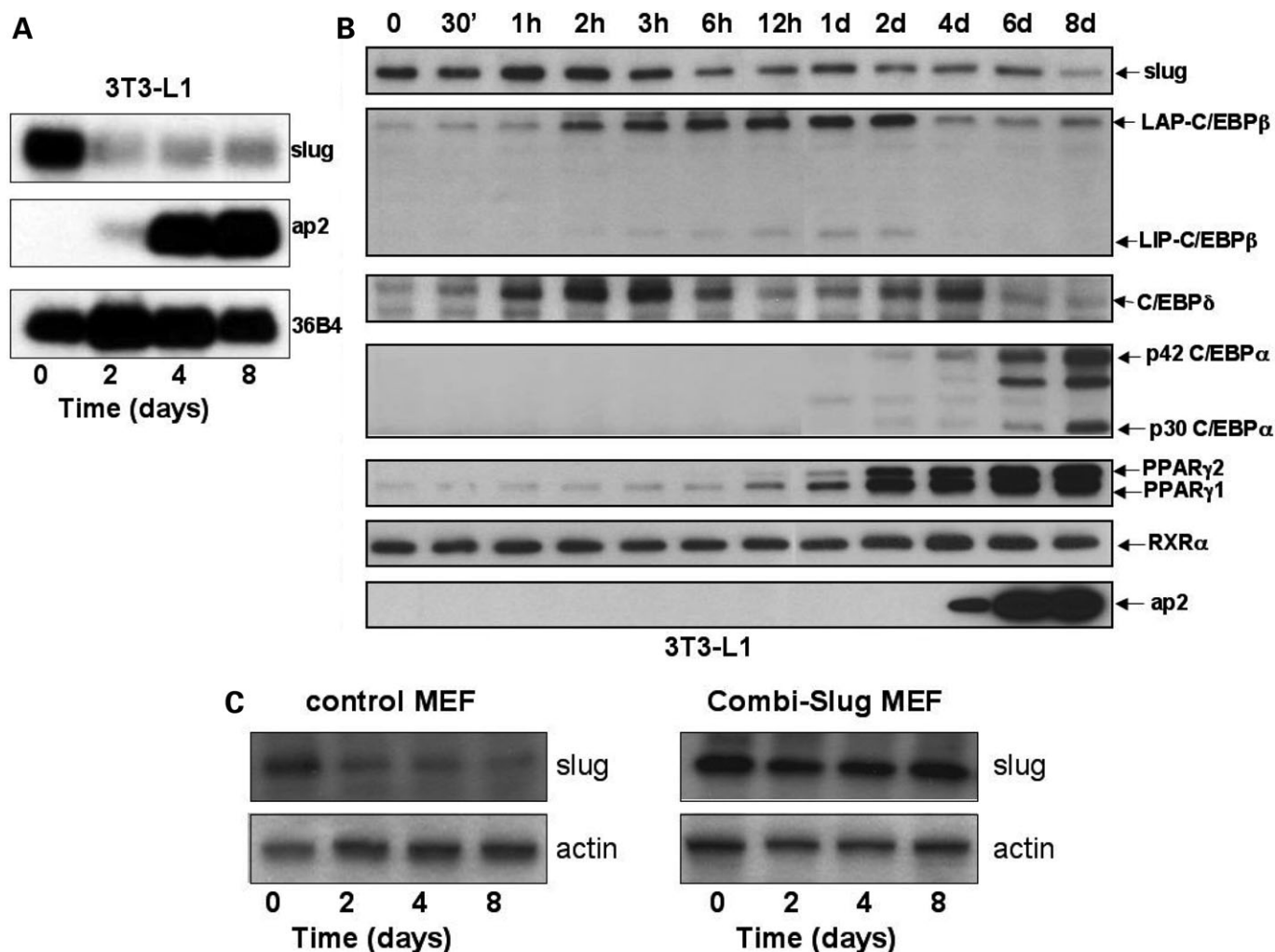


**Figure 2.** Time course of the expression of Slug during differentiation of preadipocytes. 3T3-L1 cells incubated for the indicated times after the onset of exposure to inducers of differentiation were subjected to Northern blot analysis (A), or to immunoblot analysis (B). After exposure to a hormonal cocktail, CEBP $\beta$  is actively expressed and then begins to diminish around day 2 of hormonal induction, at which point the expression of C/EBP $\alpha$  and PPAR $\gamma$  increases (23). C/EBP $\alpha$  and PPAR $\gamma$  induce programs of gene expression leading to the differentiation of mature adipocytes (2,17,24). It has been documented that selective disruption of PPAR $\gamma$ 2 impairs the development of adipose tissue and is absolutely required for differentiation (16), while C/EBP $\alpha$  is not strictly required for adipogenesis (25). These data are representative of three independent experiments. (C) Time course of Slug expression during adipocyte differentiation in control and Combi-Slug MEFs. MEFs cells incubated for the indicated time after the onset of exposure to inducers of differentiation were subjected to immunoblot analysis.

expression during the course of adipocyte differentiation in Combi-Slug cells (Fig. 2C).

The above results support the hypothesis that Slug expression modulates adipose tissue mass. Therefore, abolition of Slug overexpression might be expected to either halt or reduce WAT increase. To assess this, 12 Combi-Slug mice with an increase in the body weight when compared with wild-type mice were evaluated for WAT size following administration of tetracycline (4 g/l in the drinking water for 3 weeks, a dose sufficient to suppress exogenous Slug expression, Fig. 6A). Eleven out of 12 CombiTA-Slug mice exhibited a decrease in the body weight, being the WAT weight of these mice after tetracycline treatment similar to wild-type mice (Fig. 6B). Thus, these results indicate that the WAT alterations, induced by Slug, are reversible.

#### Expression of adipogenic genes in WAT of Slug-deficient and Combi-Slug mice

The development of adipose tissue involves a differentiation switch that activates a new programme of gene expression, followed by accumulation of lipids in a hormone-sensitive manner (1,2). To further explore the molecular basis through which Slug favours and lack of Slug impairs the development of fat tissue, we examined the expression levels of the proteins responsible for WAT development (Fig. 7A and B) and that of several adipocyte markers (Fig. 7C). As shown in Figure 7, the expression of RXR $\alpha$ , C/EBP $\delta$ , C/EBP $\beta$ , C/EBP $\alpha$  and the fat cell markers seems not to be affected. However, the expression of PPAR $\gamma$ 2 was decreased in the WAT of Slug-deficient mice and increased in the WAT of Combi-Slug mice (Fig. 7B).

**Table 1.** Adipose tissue mass in Slug-deficient and Slug-overexpressing mice

	Kidney	Reproductive fatpad	Inguinal fatpad	Retroperitoneal fatpad
<b>Male</b>				
Wild-type	0.147 ± 0.009	0.78 ± 0.13	0.56 ± 0.10	0.30 ± 0.08
Slug <sup>-/-</sup>	0.149 ± 0.005	0.11 ± 0.07	0.11 ± 0.12	0.06 ± 0.03
Combi-Slug	0.148 ± 0.008	1.75 ± 0.21	1.39 ± 0.13	0.77 ± 0.05
Slug <sup>-/-</sup> × Combi-Slug	0.148 ± 0.006	0.64 ± 0.19	0.47 ± 0.17	0.29 ± 0.05
<b>Female</b>				
Wild-type	0.143 ± 0.007	ND	0.55 ± 0.07	0.38 ± 0.09
Slug <sup>-/-</sup>	0.141 ± 0.009	ND	0.09 ± 0.10	0.08 ± 0.07
Combi-Slug	0.144 ± 0.004	ND	1.44 ± 0.17	0.89 ± 0.11
Slug <sup>-/-</sup> × Combi-Slug	0.143 ± 0.005	ND	0.49 ± 0.13	0.35 ± 0.10

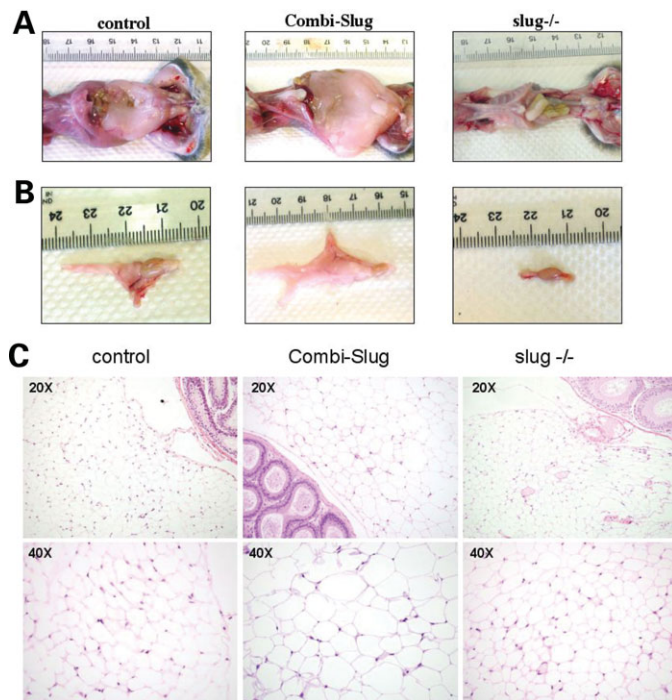


**Figure 3.** Comparison of WAT samples in Slug-deficient, Combi-Slug and control mice. (A) A ventral view of Slug-deficient, Combi-Slug and control mice (upper row). (B) A comparison of reproductive fat pads of Slug-deficient, Combi-Slug and control mice (second row). (C) Haematoxylin/eosin stained sections of reproductive fat pads from male Slug-deficient, Combi-Slug and control mice (third row, 20×; and fourth row, 40×).

Taken together, these results suggest that Slug could modulate WAT development by affecting PPAR $\gamma$ 2 expression.

#### Impaired *in vitro* adipogenesis of Slug-deficient and Combi-Slug MEFs

The adipogenesis of MEFs by hormonal induction is a well-established model system for the study of adipocyte differentiation *in vitro* (17,18). To further examine the contribution of Slug to adipogenesis, we isolated MEFs from days 13.5 of Slug<sup>-/-</sup>, Combi-Slug and control embryos (Fig. 8A). At day 8 after hormonal induction, there is lipid accumulation, defined as percentage of cells that are Oil-Red-O positive, in control MEFs (15–25%). However, there was extensive

accumulation in Combi-Slug MEFs (35–45%) and barely any lipid accumulation in Slug-deficient MEFs (0.1–0.5%) (Fig. 8B). In agreement with these morphological changes, the marker of adipogenesis, PPAR $\gamma$ 2, was also significantly reduced in the hormone-induced Slug<sup>-/-</sup> MEFs (Fig. 9A and B) and increased in Combi-Slug MEFs, compared with those in Slug<sup>+/+</sup> MEFs. This increase in PPAR $\gamma$ 2 expression was reverted upon doxycycline treatment of Combi-Slug MEFs (Fig. 9B). Similarly, the expression of the fat cell marker, ap2, confirmed the morphological changes (Fig. 9C and D). To define whether the estimation of PPAR $\gamma$  can rescue adipogenesis in Slug-deficient cells, adipocytic differentiation was induced in Slug<sup>-/-</sup> MEFs in the presence of the PPAR $\gamma$  ligand troglitazone. Of interest, the impaired adipocyte differentiation block in Slug-deficient MEFs was normalized by treatment with the PPAR $\gamma$  agonist troglitazone (Fig. 9D and E). These results suggest that Slug modulates adipogenesis *in vitro* by affecting PPAR $\gamma$ 2 expression.

#### Adipogenesis defects in Slug<sup>-/-</sup> MEFs can be rescued by ectopic expression of Slug

Our data revealed that PPAR $\gamma$ 2 expression is modulated by Slug, suggesting an interesting link between this gene and Slug. In order to confirm this transcriptional regulation, we re-introduced wild-type Slug in Slug-deficient MEFs by retroviral transduction and evaluated the expression level of PPAR $\gamma$ 2 by quantitative real-time PCR. Retrovirus-mediated expression of Slug in Slug-deficient MEFs re-established the aberrant expression of PPAR $\gamma$ 2 and adipocyte differentiation capacity to wild-type levels, as shown in Figure 10A–D. The demonstration that Slug was sufficient to normalize the adipocyte differentiation capacity of Slug-deficient cells and to fully recover PPAR $\gamma$ 2 expression in cells lacking Slug further indicates that PPAR $\gamma$ 2 was regulated directly by Slug.

#### Slug does not transactivate the PPAR $\gamma$ 2 promoter

Because the results so far suggest that Slug directly regulates PPAR $\gamma$ 2 expression, we examined whether Slug might be directly involved in the control of PPAR $\gamma$ 2 transcription. A 1 kb proximal promoter region of human PPAR $\gamma$ 2 was previously shown to be sufficient to drive the PPAR $\gamma$ 2's expression in reporter assays (19), and it is active in U2OS cells when co-transfected with C/EBP $\alpha$  and C/EBP $\beta$  expression vectors

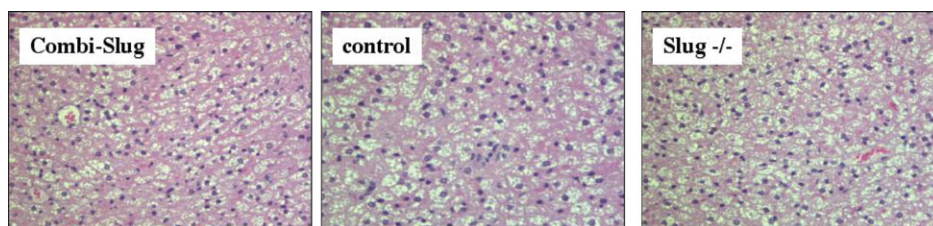


**Figure 4.** A comparison of BAT samples in Slug-deficient, Combi-Slug and control mice. Haematoxylin/eosin stained sections of interscapular brown fat from Slug-deficient, Combi-Slug and control mice (20 $\times$ ).

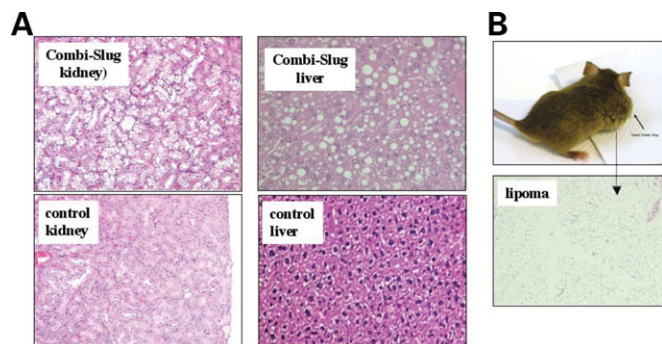


**Figure 5.** Lipid accumulation in Combi-Slug mice. (A) Haematoxylin-eosin stained sections of the liver and kidney tissues coming from wild-type and Combi-Slug mice. (B) Tumour and histologic appearance of a lipoma developed in CombiTA-Slug mice after Haematoxylin-eosin staining.

(Fig. 11). To directly assess the ability of Slug to activate transcription from DNA sequences present in the PPAR $\gamma$ 2 promoter, an expression vector containing a *Slug* cDNA was co-transfected into U2OS cells along with the reporter vector containing the PPAR $\gamma$ 2 promoter (pGL3-hPPARg2p1000 vector). Co-expression of *Slug* did not increase luciferase activity when compared with the activity with the empty vector (Fig. 11).

### Histone modifications in WAT of Combi-slug and Slug-deficient mice

The above results suggest that Slug does not have a direct role in inducing expression of PPAR $\gamma$ 2 through association with regulatory elements in the PPAR $\gamma$ 2 gene promoter, although only the 1 kb promoter region was tested. However, programmed regulation of gene expression is the result of coordinated modulation of the transcription machinery and chromatin-remodelling factors, notably histone acetylation and deacetylation. To address this issue, we measured the histone acetylation status in WAT of Combi-Slug and Slug-deficient mice. We analysed the acetylation levels at histone H3 using protein blotting. We found a high increase in histone H3 acetylation in Combi-Slug WAT and a decrease in histone H3 acetylation in Slug  $-/-$  WAT, compared with control mice (Fig. 12). Thus, these results show a correlation between SLUG expression and histone acetylation status in adipose tissue.

Recent work has implicated HDAC as mediators of the gene regulation modulated by Slug (20,21). The major function of HDAC is to remove acetyl groups from histones, which results in condensation of the chromatin structure (22). This,

in turn, diminishes the access of transcription factors to the target DNA and ultimately leads to transcriptional repression. To explore whether Slug is indeed recruited at the PPAR $\gamma$ 2 gene promoter inside the cell nucleus, we performed a ChIP assay (Fig. 13A–C). Chromatin samples were prepared from WAT of control, Combi-Slug and Slug-deficient mice and then immunoprecipitated with specific antibodies against C/EBP $\alpha$ , Slug and HDAC1. The binding of C/EBP $\alpha$  was detectable, which is consistent with the current model of PPAR $\gamma$ 2 control by C/EBPs (Fig. 13B). This ChIP analysis revealed that both Slug and HDAC1 are recruited at the PPAR $\gamma$ 2 promoter in control adipose tissue (Fig. 13B). Importantly, HDAC1 is not recruited at the PPAR $\gamma$ 2 promoter in WAT cells from Combi-Slug mice, in agreement with the abundance of acetylated histones at WAT of Combi-Slug mice (Fig. 12). In contrast, HDAC1 is recruited in the PPAR $\gamma$ 2 promoter in Slug-deficient WAT (Fig. 13B). Thus, these data show a differential HDAC recruitment to the PPAR $\gamma$ 2 promoter in a tissue- and Slug-dependent manner. These findings predict that increased Slug expression may also lead to increased acetylation at the PPAR $\gamma$ 2 promoter and vice versa. To test this, we determined histone H3 acetylation at the PPAR $\gamma$ 2 promoter in WAT of control, Combi-Slug and Slug-deficient mice (Fig. 13D). The ChIP analysis showed a differential H3 acetylation at the PPAR $\gamma$ 2 promoter in a Slug-dependent manner, suggesting a change in the PPAR $\gamma$ 2 chromatin towards a more active and ‘open’ state in the Combi-Slug WAT and towards an inactive state in the Slug-deficient WAT. If this were the case, then C/EBPs might be expected to be less able to transactivate the PPAR $\gamma$ 2 reporter in the absence of Slug. To directly assess this, an expression vector containing either a C/EBP $\alpha$  or a C/EBP $\beta$  cDNA was co-transfected into Slug-deficient cells along with the reporter vector containing the PPAR $\gamma$ 2 promoter (pGL3-hPPARg2p1000 vector). Co-expression of C/EBP $\alpha$  or C/EBP $\beta$  increased luciferase activity when compared with the activity with the empty vector, although they were not very efficient (Fig. 13E). However, co-expression of Slug was able to increase the luciferase activity induced by C/EBP $\alpha$  or C/EBP $\beta$  (Fig. 13E). These observations may explain the differences in PPAR $\gamma$ 2 expression in Slug-deficient and Combi-Slug mice and the role of Slug in WAT development.

### DISCUSSION

In mammals, cell specification is a process in which cells first become committed to a developmental fate, after which they

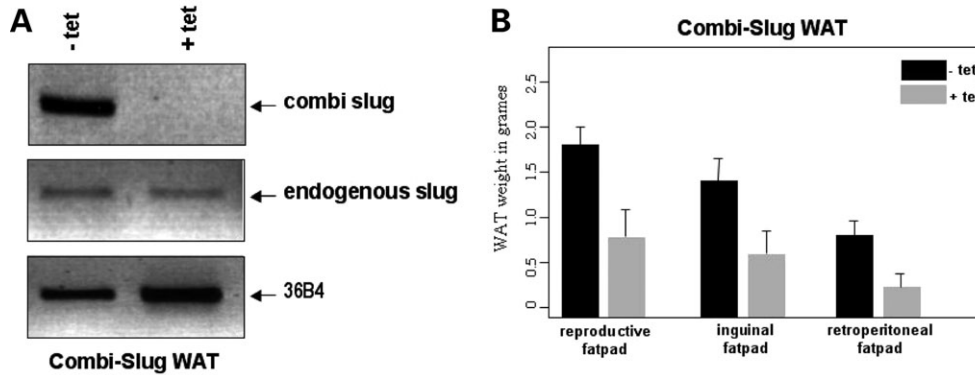


**Figure 6.** WAT size in CombiTA-Slug mice after suppression of Slug expression by tetracycline treatment. (A) Analysis of tetracycline-dependent Slug expression in inguinal fatpad for CombiTA-Slug (-tet, +tet in water) by RT-PCR. Mice were 6 months old. 36B4 was used to check cDNA integrity and loading. (B) WAT weights in CombiTA-Slug mice ( $n=12$ ) after suppression of Slug expression by tetracycline treatment (4 gr/l) for 3 weeks. Differences were statistically significant ( $P<0.01$ ) as determined by Mann-Whitney's test. WAT mass was not affected in control mice under tetracycline treatment (4 gr/l) for 3 weeks.

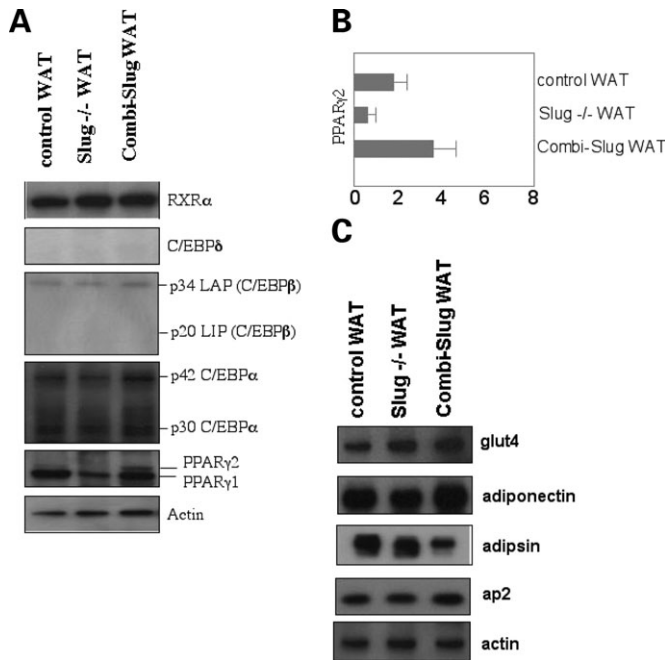


**Figure 7.** Adipogenic gene expression in Slug-deficient and Combi-Slug WAT. (A) Western blot analyses of regulators of adipocyte function in WAT of Slug-deficient mice, control mice and Combi-Slug mice. (B) Quantification of *PPARγ2* expression by real-time PCR in WAT of Slug-deficient mice, control mice and Combi-Slug mice ( $n=3$ ). Percentage of *PPARγ2* transcripts with reference to b-actin is shown. Differences were statistically significant ( $P<0.03$ ) as determined by Mann-Whitney's test. (C) Western blot analyses of fat cell markers such as *glut4*, *adiponectin*, *adipsin*, and *ap2* in WAT of Slug-deficient mice, control mice and Combi-Slug mice. These data are representative of three independent experiments.

differentiate and acquire the properties of a specific cell type. Adipocyte development is controlled by a genetic programme that leads fibroblasts to become pre-adipocytes. When further induced, pre-adipocytes differentiate and express genes that allow them to store lipid and become mature adipocytes. Although many of the components of the gene regulatory network that controls differentiation of adipocytes have been

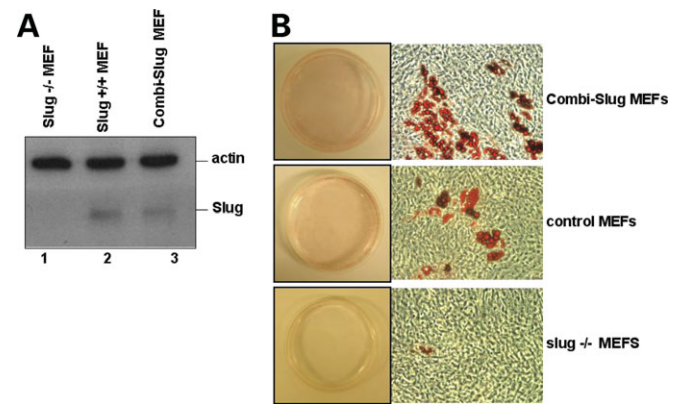


**Figure 8.** Altered lipid accumulation in Slug-deficient and Combi-Slug MEFs. (A) Western-blot analyses of Slug expression in control, Slug-deficient and Combi-Slug MEFs before exposure to inducers of differentiation. Actin was used to check protein loading. (B) Primary embryonic fibroblasts from each line were cultured in the presence of standard differentiation induction medium. At day 8 after induction of adipocyte differentiation, cells were fixed and stained for neutral lipids with Oil Red O. The original magnification is  $\times 20$ . This experiment was repeated three times using cells prepared from all lines and from different embryos and similar results were obtained. These data are representative of three independent experiments.

elucidated in studies of cultures 3T3-L1, little is known about the developmental signals that control the development of adipocytes *in vivo*. The present study establishes, for the first time, the important role played by SLUG in adipogenesis *in vivo* and *in vitro*.

Slug expression is tightly controlled during adipocyte differentiation. Slug is expressed *in vivo*, but is only expressed transiently in culture cells, suggesting that it may play a role in initiating and/or maintaining adipogenesis *in vivo*. Expression of Slug was observed before the induction of differentiation in 3T3-L1 cells (which are lineage-determined pre-adipocytes) and MEFs (which are uncommitted progenitor cells) and to be downregulated within the first 6 h after applying the hormonal stimuli in both cell types. A similar expression pattern is observed in the haematopoietic system in which uncommitted

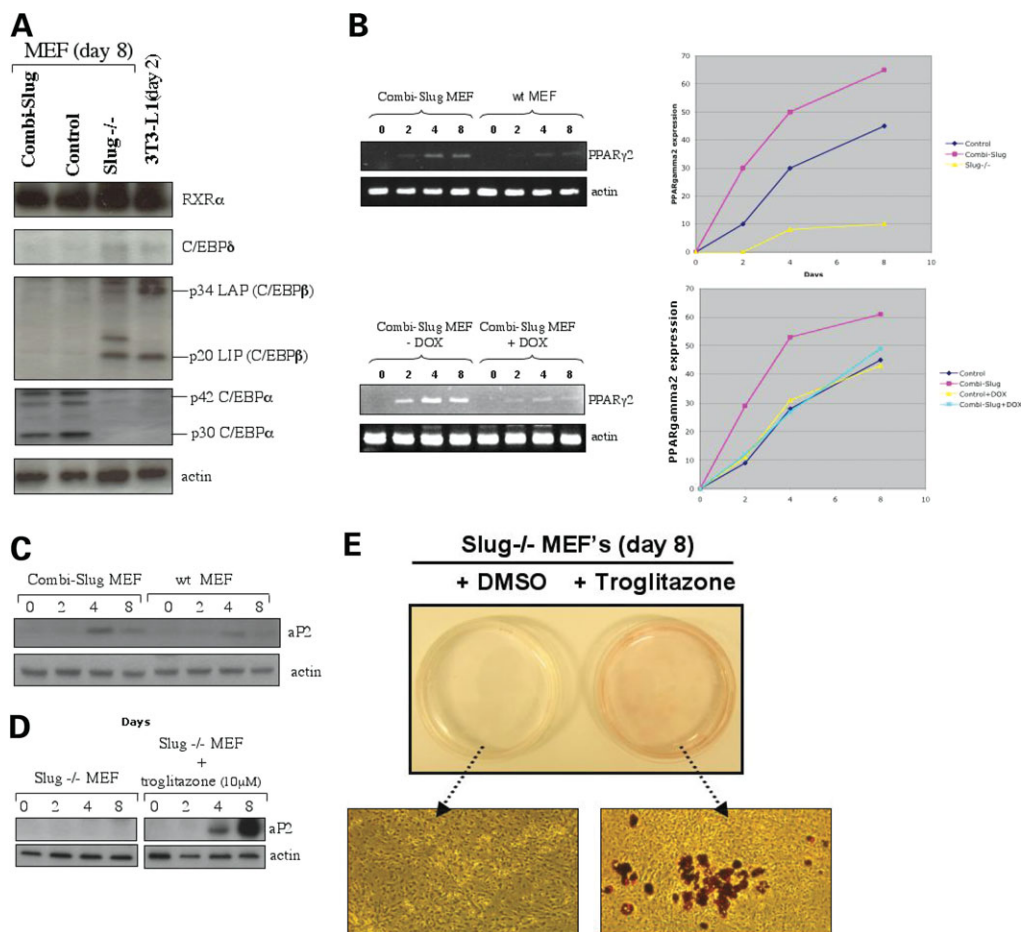


**Figure 9.** Adipogenic gene expression in Slug-deficient and Combi-Slug MEFs during differentiation. (A) Western-blot analysis of adipogenic genes at day 8 post-induction in Slug-deficient, control and Combi-Slug MEFs. 3T3-L1 cells at day 2 post-induction are used as a control. The pattern of adipogenic gene expression in Combi-Slug MEFs is similar to a terminally differentiated cell at day 8 post-induction. However, the pattern of adipogenic gene expression in Slug-deficient MEFs at day 8 post-induction is similar to 3T3-L1 cells at day 2 post-induction. (B) Quantification of *PPAR* $\gamma$ 2 expression by real-time PCR in control, Slug-deficient and combi-Slug  $\pm$  DOX MEFs at day 0, 2, 4 and 8 post-induction. A representative ethidium bromide agarose gel is shown close to the percentage of *PPAR* $\gamma$ 2 transcripts with reference to b-actin is shown. Differences were statistically significant ( $P < 0.01$ ) as determined by Mann-Whitney's test. (C) Expression of ap2 was studied by western-blot in control and Combi-Slug MEFs at day 0, 2, 4 and 8 post-induction. (D) Slug $^{-/-}$  MEFs were induced with differentiation medium in the presence or absence of 10  $\mu$ M PPAR $\gamma$  ligand troglitazone. At day 0, 2, 4 and 8 post-induction ap2 protein expression was studied by western-blot. Actin was included as a loading control. (E) At day 8, post-induction cells were stained for droplets with Oil Red O and the morphological differentiation of Slug-deficient MEFs+troglitazone is shown. These data are representative of three independent experiments.

progenitor cells differentiate to mature cells at which time, the expression of Slug is downregulated (7,8). These findings indicate that Slug downregulation is required to initiate adipogenesis, suggesting that it could play a role in the development or maintenance of these cells from precursor cells. The reduced WAT mass observed in Slug-deficient mice and the reduced adipocyte differentiation seen in Slug-deficient MEFs are also consistent with a role for Slug in early adipocyte differentiation, although the present experiments cannot distinguish function of SLUG in pre-adipocytes from an effect on lineage commitment. The dissection of the mechanisms controlling its expression could in turn lead to the identification of signals that control adipogenesis *in vivo*. Of note, Kit is one of the markers for presumptive mesenchymal stem cells as well as being an activator of Slug expression (8). Moreover, several Slug targets have been implicating in regulating stem cell function (21). The regulation of these genes by Slug

could be important in maintaining uncommitted progenitor cells.

It appears that Slug must be kept above a certain threshold level to achieve normal WAT development both *in vivo* and *in vitro*. Consistent with this interpretation, mice carrying a tetracycline-repressible Slug transgene (Combi-Slug) exhibit an increase in the WAT mass that was specifically re-established by suppression of the *Slug* transgene. Consistent with *in vivo* data, Combi-Slug MEFs increased adipocyte differentiation, suggesting that this factor positively regulates adipocyte differentiation. Thus, it seems likely that failure to regulate Slug expression explains why Combi-Slug mice develop obesity.

The data presented here indicate that SLUG is a novel mediator of adipose tissue development in mammals. We therefore analysed the molecular mechanism by which Slug controls WAT development. It is well defined that C/EBP $\beta$



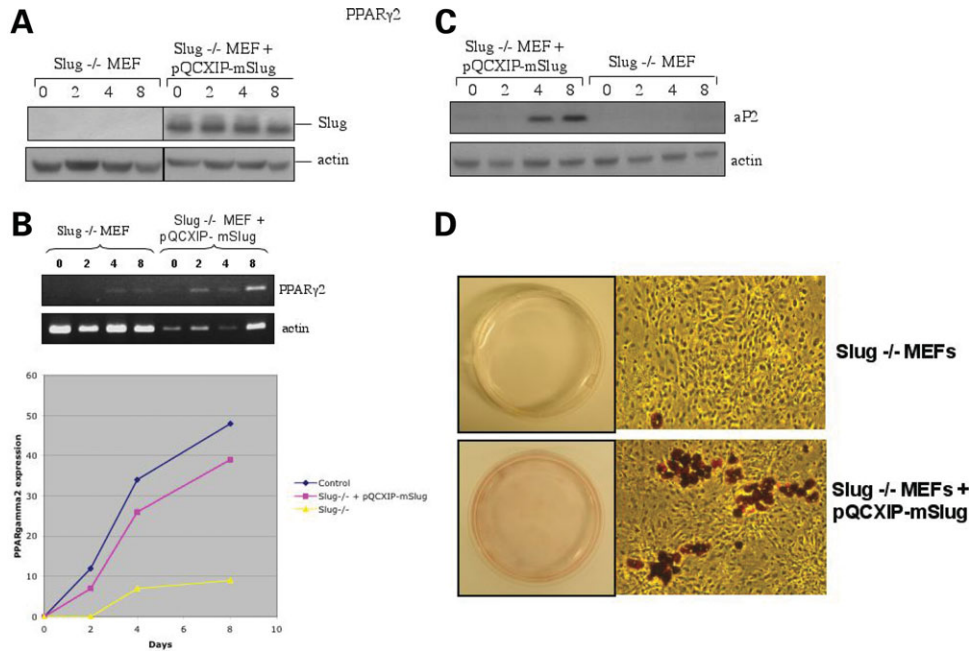


**Figure 10.** Retrovirus-mediated overexpression of Slug rescues the impaired *in vitro* adipogenesis of Slug-deficient MEFs. (A) Analysis of Slug protein by western-blot in Slug<sup>-/-</sup> MEFs infected with either a control retroviral vector or one expressing Slug (pQCXIP-mSlug) at day 0, 2, 4 and 8 after exposure to inducers of adipocyte differentiation. Actin was included as a loading control. (B) Quantification of *PPARγ2* expression by real-time PCR in Slug<sup>-/-</sup> MEFs infected with either a control retroviral vector or one expressing Slug (pQCXIP-mSlug) at day 0, 2, 4 and 8 post-induction. A representative ethidium bromide agarose gel is shown close to the percentage of *PPARγ2* transcripts with reference to β-actin is shown. Differences were statistically significant ( $P < 0.01$ ) as determined by Mann-Whitney's test. (C) Analysis of ap2 protein by western blot in Slug<sup>-/-</sup> MEFs infected with either a control retroviral vector or one expressing Slug (pQCXIP-mSlug) at day 0, 2, 4 and 8 after exposure to inducers of adipocyte differentiation. Actin was included as a loading control. (D) At day 8 after induction of adipocyte differentiation, cells were observed by light microscopy with Oil-Red-O staining (the original magnification is  $\times 20$ ). These data are representative of three independent experiments.

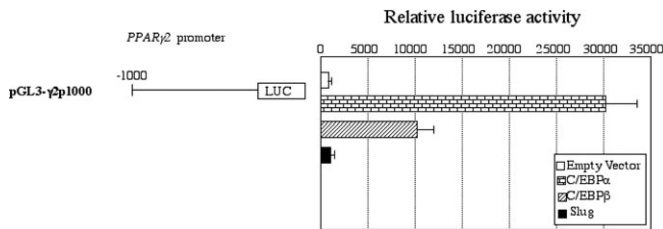


**Figure 11.** Slug does not transactivate the *PPARγ2* promoter. A 1 kb proximal promoter region of human *PPARγ2* was previously shown to be sufficient to drive the *PPARγ2*'s expression in reporter assays (19) and it is active in U2OS cells when co-transfected with C/EBPα and C/EBPβ expression vectors. To directly assess the ability of Slug to activate transcription from DNA sequences present in the *PPARγ2* promoter, an expression vector containing a *Slug* cDNA was co-transfected into U2OS cells along with the reporter vector containing the *PPARγ2* promoter (pGL3-hPPARγ2p1000 vector). Luciferase reporter assays demonstrate lack of responsiveness of the human *PPARγ2* reporter to *Slug*. The number shown at the left of the reporter construct denotes the 5'-boundaries (bp upstream of the initiation site). These data are representative of three independent experiments.

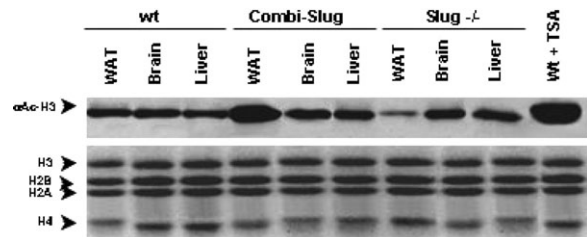


**Figure 12.** Histone acetylation status. Protein acetylation patterns of different tissue samples surgically removed from different wild-type, Slug-deficient and Combi-Slug mice. Data show high increase in histone H3 acetylation in Combi-Slug WAT and decrease in histone H3 acetylation in Slug<sup>-/-</sup> WAT compared with wt mice. Brain and liver were used as negative upregulation profile. Samples were blotted with anti-acetyl histone H3 (Upstate Biotechnology). Wild type tissue from a Histone Deacetylase inhibitor (HDACi) treated mouse was used as a positive upregulation and Acetylated H3-increased sample. Core H3 coomassie stained was used as loading control. These data are representative of three independent experiments.

can promote the fat differentiation of culture cells. After exposure to a hormonal cocktail, CEBPβ is actively expressed and then begins to diminish around day 2 of hormonal induction, at which point the expression of C/EBPα and PPARγ increases (23). C/EBPα and PPARγ induce programmes of gene expression, leading to the differentiation of mature adipocytes (2,17,24). It has been documented that selective disruption of PPARγ2 impairs the development of adipose

tissue and is absolutely required for differentiation (16), whereas C/EBPα is not strictly required for adipogenesis (25). *In vivo* and *in vitro* Combi-Slug and Slug-deficient tissues and MEFs exhibit normal expression of C/EBP φαχτορ. However, we found that PPARγ2 expression is altered both *in vivo* in WAT of Slug-deficient and Combi-Slug mice and *in vitro* in Slug-deficient MEFs and Combi-Slug MEFs during the course of adipocytic differentiation. Complementation studies in Slug-deficient MEFs confirmed

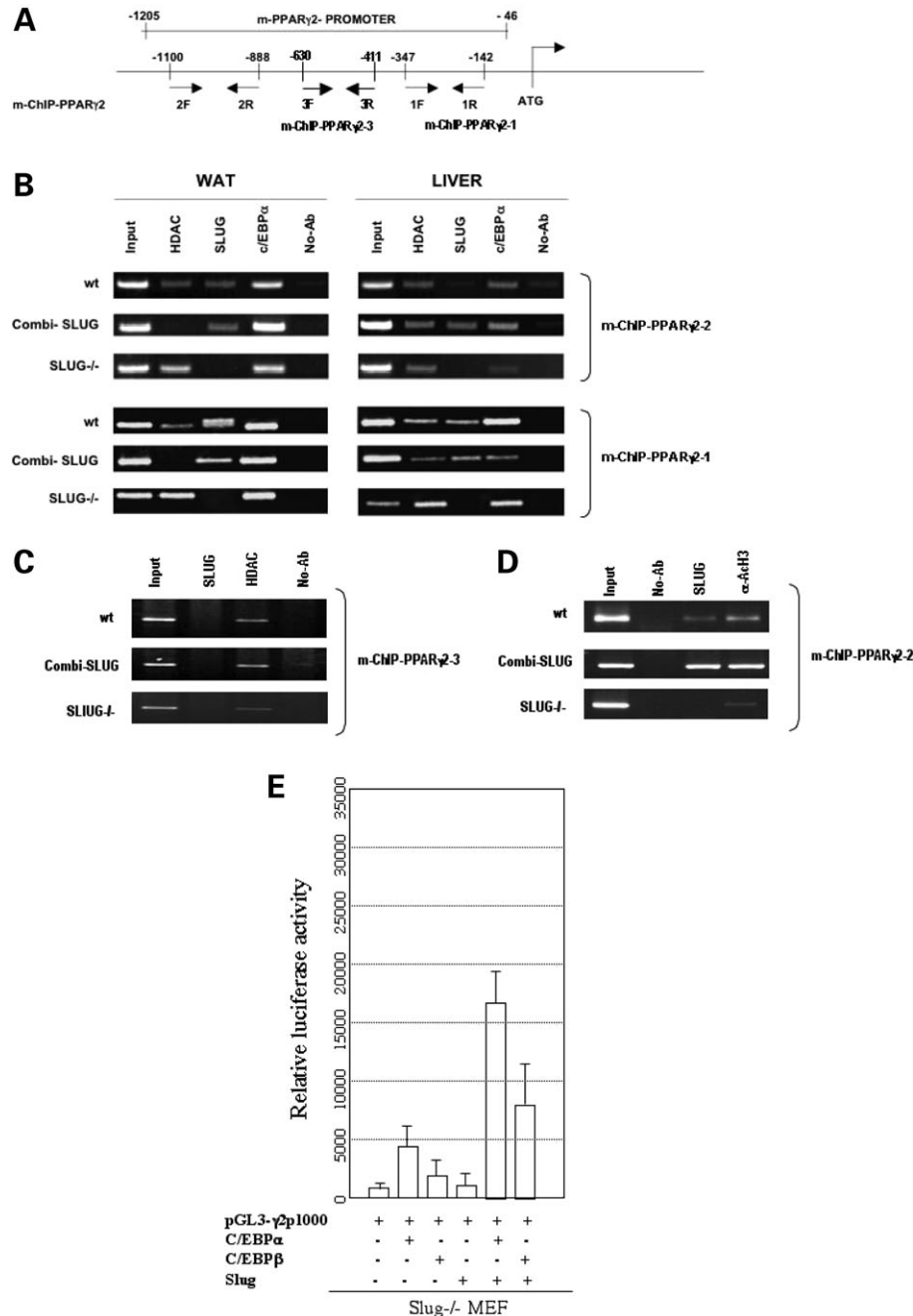


**Figure 13.** Recruitment analysis of HDAC, SLUG and c/EBP $\alpha$  to mouse PPAR $\gamma$ 2 gene promoter. (A) Schematic depiction of the mouse PPAR $\gamma$ 2 promoter sequence from  $-1205$  to  $-46$  (GenBank: AY243584), with arrows indicating the forward and reverse primers used to amplify ChIP products. Pairs of primers 1 and 2 are around two Slug DNA-binding sites, and pairs of primer 3 are not around Slug DNA-binding sites. (B) WAT and Liver ChIP from different mice (*wt*, *Combi-SLUG* and *SLUG* $^{-/-}$ ) using polyclonal anti-HDAC1 (H-51), anti-SLUG (H-140) or anti-c/EBP $\alpha$  (14AA) from Santa Cruz Biotechnology Inc. Data show a differential HDAC recruitment to the PPAR $\gamma$ 2 promoter in a tissue- and genetic background-dependent manner. The presence of the promoter DNA before immunoprecipitation was confirmed by PCR (Input). C/EBP $\alpha$  was used as a positive response element from PPAR $\gamma$ 2 gene promoter. PCR products were resolved in 2% agarose gels containing ethidium bromide. (C) WAT ChIP from different mice (*wt*, *Combi-SLUG* and *SLUG* $^{-/-}$ ) using polyclonal anti-HDAC1 (H-51), or anti-SLUG (H-140) from Santa Cruz Biotechnology Inc. Data show no Slug recruitment to the PPAR $\gamma$ 2 promoter using pairs of primers that are not around Slug DNA-binding sites. The presence of the promoter DNA before immunoprecipitation was confirmed by PCR (Input). PCR products were resolved in 2% agarose gels containing ethidium bromide. (D) WAT ChIP from different mice (*wt*, *Combi-SLUG* and *SLUG* $^{-/-}$ ) using anti-acetyl histone H3 (Upstate Biotechnology) or anti-SLUG (H-140) from Santa Cruz Biotechnology Inc. Data show a correlation between Slug expression and H3 acetylation at the PPAR $\gamma$ 2 promoter. The presence of the promoter DNA before immunoprecipitation was confirmed by PCR (Input). PCR products were resolved in 2% agarose gels containing ethidium bromide. (E) C/EBP $\alpha$  and C/EBP $\beta$  ability to transactivate the PPAR $\gamma$ 2 promoter in Slug-deficient cells. To directly assess the ability of C/EBP $\alpha$  and C/EBP $\beta$  to activate transcription from DNA sequences present in the PPAR $\gamma$ 2 promoter in Slug-deficient cells, C/EBP $\alpha$  and C/EBP $\beta$  expression vectors were co-transfected into Slug $^{-/-}$  MEF along with the reporter vector containing the PPAR $\gamma$ 2 promoter (pGL3-hPPAR $\gamma$ 2p1000 vector) in the presence (+) and in the absence (-) of Slug. Luciferase reporter assays demonstrate an efficient responsiveness of the human PPAR $\gamma$ 2 reporter to C/EBP $\alpha$  and C/EBP $\beta$  in the presence of Slug. These data are representative of three independent experiments.

this regulation, although Slug was not able to activate transcription from a reporter vector containing the PPAR $\gamma$ 2 promoter. However, when we measured the histone acetylation status in WAT of Combi-Slug and Slug-deficient mice, we identified a correlation between Slug gene expression and histone acetylation status in adipose tissue. This observation, close to recent work implicating HDAC as mediators of the gene regulation modulated by Slug (20,21), prompted us to explore whether Slug is indeed recruited at the PPAR $\gamma$ 2 gene promoter. Our ChIP experiments showed that Slug and HDAC1 were bound to the endogenous PPAR $\gamma$ 2 promoter in intact chromatin in WAT and identified a differential HDAC recruitment to the PPAR $\gamma$ 2 promoter in a tissue- and Slug-dependent manner. In agreement with these observations, the ChIP analysis confirmed a differential H3 acetylation at the PPAR $\gamma$ 2 promoter in a Slug-dependent manner. Thus, the most straightforward model for the Slug requirement for PPAR $\gamma$ 2 gene expression would be that lack of Slug binding to the PPAR $\gamma$ 2 gene results in the formation of a silencing complex that represses the expression of the gene by histone deacetylation. In contrast, HDAC1 is not recruited at the PPAR $\gamma$ 2 promoter in WAT cells from Combi-Slug mice, in agreement with the abundance of acetylated H3 histones at WAT of Combi-Slug mice (Figs 12 and 13D). This, in turn, will increase the access of transcription factors to the target DNA and ultimately leads to PPAR $\gamma$ 2 transcriptional activation (Fig. 13E). This could be a potentially relevant clinical issue, as HDAC inhibitors are drugs that have activity at doses that are well tolerated by patients in clinical trials (26). In agreement with this model, it has been shown that downregulation of HDACs stimulates adipocyte differentiation (27).

The expression of SLUG in human WAT tissue is of relevance in human obesity, particularly when the obesity observed in Combi-Slug mice is associated with adipose cell hypertrophy; the WAT size in Combi-Slug mice can be reverted by suppressing Slug expression and the WAT size is reduced in Slug-deficient mice. SLUG is overexpressed in other human diseases such as cancer (10,28,29). Although white fat is a non-malignant tissue, it has the capability to quickly proliferate and expand (30,31). Thus, SLUG expression might therefore define a common pathway for cancer and obesity. However, the role conferred by Slug is reversible in obesity.

Slug has been shown to play roles similar to Snail in several systems, and, thus, other members of the Snail family of transcription factors could also be involved in biological functions similar to those described herein to Slug (32). However, it is not clear whether this functional equivalence also occurs during adipogenesis. Among previously identified Slug-regulated species, the related transcription factor Snail was reported as Slug induced in *Xenopus* (33). However, Slug does not influence the expression of Snail in MDCK cells (34) and in MEFs (21). Similarly, we did not detect a change in Snail expression associated with overexpression or deficiency of Slug in mice.

In summary, we report the identification of Slug as playing an essential role in adipose tissue development and differentiation. An analysis of its regulation *in vivo* could lead to a full understanding of regulation of adipogenesis. Our results

connect adipogenesis with the requirement of a critical level of an epithelial–mesenchymal transition regulator in mammals. Because Slug modulates adipose tissue mass in mice and is also expressed in human white fat, these results will help to develop a strategy that would form the basis for improved antiobesity and antilipodystrophy therapies.

## MATERIALS AND METHODS

### Mice

Animals were housed under non-sterile conditions in a conventional animal facility. Slug-deficient and Combi-Slug mice have been described previously (35). Combi-Slug mice are analysed on a wild-type background unless otherwise specified. Combi-Slug $\times$ Slug $^{-/-}$  mice were generated as follow: heterozygous Slug $+/-$  mice were bred to Combi-Slug transgenic mice to generate compound heterozygotes; F1 animals were crossed to obtain null Slug $-/-$  mice heterozygous for Combi-Slug transgenic mice as described (10). The animals were maintained regular chow diet, unless otherwise specified. All experiments were performed according to the relevant regulatory standards.

### Histological analysis

All tissue samples were closely examined under the dissecting microscope and processed into paraffin, sectioned and examined histologically. All tissue samples were taken from homogeneous and viable portions of the resected sample by the pathologist and fixed within 2–5 min of excision. Haematoxylin- and eosin-stained sections of each tissue were reviewed by a single pathologist (T.F.). For comparative studies, age-matched mice were used.

### Preparation of primary MEFs

Heterozygous Slug $+/-$  mice were crossed to obtain wild-type and null Slug $-/-$  embryos. Primary embryonic fibroblasts were harvested from 13.5 d.p.c. embryos. Head and organs of day 13.5 embryos were dissected; foetal tissue was rinsed in phosphate-buffered saline (PBS), minced and rinsed twice in PBS. Foetal tissue was treated with trypsin/EDTA and incubated for 30 min at 37°C and subsequently dissociated in medium. After removal of large tissue clumps, the remaining cells were plated out in a 175 cm<sup>2</sup> flask. After 48 h, confluent cultures were frozen down. These cells were considered as being passage 1 MEFs. For continuous culturing, MEF cultures were split 1:3. MEFs and the  $\phi$ NX ecotropic packaging cell line were grown at 37°C in Dulbecco's modified Eagle's medium (DMEM; Boehringer Ingelheim) supplemented with 10% heat-inactivated foetal bovine serum (FBS) (Boehringer Ingelheim). All the cells were negative for mycoplasma (MycAlert<sup>TM</sup> Mycoplasma Detection Kit, Cambrex).

### Adipocyte differentiation

3T3-L1 pre-adipocytes were cultured as described previously (24). Wild-type, Combi-slug and slug $^{-/-}$  MEFs were cultured

at 37°C in standard D-MEM:F12 medium (Gibco) supplemented with 10% heat-inactivated FBS (Hyclone), 100 U/ml penicillin (Biowhittaker) and 100 µg/ml streptomycin (Biowhittaker). About 10<sup>6</sup> cells of each genotype were plated to 10 cm plastic dishes and propagated to confluence. Two days after confluence, the adipocyte differentiation programme was induced by feeding the cells with standard medium supplemented with 0.5 mM 3-isobutyl-1-Methylxanthine (Sigma), 1 µM dexamethasone (Sigma) and 5 µg/ml insulin (Sigma) for 2 days, and then, with standard medium supplemented with 5 µg/ml insulin for 6 days. This medium was renewed every 2 days. Troglitazone (Calbiochem), or vehicle, was used at 10 µM during the 8 days of differentiation when required. After 8 days, the appearance of cytoplasmic lipid accumulation was observed by Oil-Red-O staining. Lipid accumulation was defined as percentage of cells that were Oil-Red-O positive by counting approximately 700 cells in at least three independent replicates for each experiment. Briefly, cells were washed with PBS, and then fixed with 3.7% formaldehyde for 2 min. After a wash with water, cells were stained with 60% filtered Oil-Red-O stock solution [0.5 g of Oil-Red-O (Sigma) in 100 ml of isopropanol] for 1 h at room temperature. Finally, cells were washed twice in water and photographed. To prepare RNA for northern blotting and proteins for western blotting, cells were harvested at days 0, 2, 4 and 8 of differentiation.

### RNA extraction

Total RNA was isolated in two steps using TRIzol (Life Technologies, Inc., Grand Island, NY, USA), followed by Rneasy Mini-Kit (Qiagen Inc., Valencia, CA, USA) purification following manufacturers' RNA Clean-up protocol with the optional On-column DNase treatment. The integrity and the quality of RNA were verified by electrophoresis and its concentration measured.

### Reverse transcription-PCR

Human WAT samples were obtained from Zen-bio [hWAT#1 is Cat. number RNA-T10-1 with a body mass index (BMI) of 21.23; hWAT#2 is Cat. number RNA-T10-2 with a BMI of 27.27 and hWAT#3 is Cat. number RNA-T10-3 with a BMI of 32.55]. To analyse expression of CombitA-*Slug* and endogenous *Slug* in mouse cell lines and mice, RT was performed according to manufacturer's protocol in a 20 µl reaction containing 50 ng of random hexamers, 3 µg of total RNA and 200 U of Superscript II RNase H<sup>-</sup> RT (Gibco/BRL). The sequences of the specific primers were as follows: Combi-polyA-B1: 5'-TTGAGTGCATTCTAGTTGTG-3'; mSlugF: 5'-GTTTCAGTGCAATTTATGCAA-3' and mSlugB: 5'-TTA-TACATACTATTTGGTTG-3'. To analyse expression of human *SLUG*, the thermocycling parameters for the PCR reactions and the sequences of the specific primers were as follows: 30 cycles at 94°C for 1 min, 56°C for 1 min and 72°C for 2 min; sense primer 5'-GCCTCCAAAAGCCAACTA-3' and anti-sense primer 5'-CACAGTGATGGGGCTGTATG-3'. The PCR products were confirmed by hybridization with specific probes. Amplification of  $\alpha 2 \text{ av} \delta$  36B4 served as a control to

assess the adipose tissue and the quality of each RNA sample, respectively.

### Real-time PCR quantification

Real-time quantitative PCR was developed and carried out in human WAT samples obtained from Zen-bio (hWAT#1, hWAT#2 and hWAT#3) for the detection and quantitation of the *SLUG* expression. The PCRs were set up in a reaction volume of 50 µl using the TaqMan PCR Core Reagent kit (PE Biosystems). PCR primers were synthesized by Isogen. Each reaction contained 5 µl of 10× buffer; 300 nM each amplification primer; 200 µM each dNTP and 1.25 U AmpliTaq Gold, 2 mM MgCl<sub>2</sub> and 10 ng cDNA. cDNA amplifications were carried out in a 96-well reaction plate in a PE Applied Biosystems 5700 Sequence Detector. Thermal cycling was initiated with a first denaturation step of 10 min at 95°C. The subsequent thermal profile was 40 cycles of 95°C for 15 s, 55°C for 30 s and 72°C for 1 min. Multiple negative water blanks were tested and a calibration curve determined in parallel with each analysis. Although equal amounts of cDNA were used, a  $\beta$ -actin endogenous control was included to relate *SLUG* expression to total cDNA in each sample.

Similarly, a real-time quantitative PCR was developed and carried out in control, *Slug* <sup>-/-</sup> and Combi-*Slug* WAT samples for the detection and quantitation of the *PPAR* $\gamma$ 2 expression. Thermocycling was carried out for 40 cycles in triplicate. Each cycle consisted of 94°C for 15 s, 56°C for 30 s and 72°C for 30 s. *PPAR* $\gamma$ 2 primers were HMPPARG2-F: 5'-atgggtgaaactctggag-3' and HMPPARG2-B: 5'-ccttgatcctcacaagc-3'.

### Northern blot analysis

Total cytoplasmic RNA (10 µg) of 3T3-L1 cells harvested at days 0, 2, 4 and 8 of differentiation was glyoxylated and fractionated in 1.4% agarose gels in 10 mM Na<sub>2</sub>HPO<sub>4</sub> buffer (pH 7.0). After electrophoresis, the gel was blotted onto Hybond-N (Amersham), UV-crosslinked and hybridized to <sup>32</sup>P-labelled mouse *Slug* and *ap2* probes, respectively. Loading was monitored by reprobing the filter with a mouse 36B4 probe.

### Retroviral infection

*Slug*-deficient MEFs were infected with high-titres retrovirus stocks produced by transient transfection of  $\phi$ NX cells. The efficiency of infection was always >80% (data not shown). The day before the infection, cells were plated at 2 × 10<sup>6</sup> cells per 10 cm dish. Infected MEFs were selected for 3 days with 2.5 µg/ml of puromycin (Sigma) and replated for the corresponding assay. The mouse *Slug* cDNA was subcloned in the pQCXIP retrovirus (obtained from T. Jacks, Massachusetts Institute of Technology), as described previously (21).

### Western blot analysis

Western blot analysis of different cells and tissues was carried out essentially as described (36). Extracts were normalized for protein content by Bradford analysis (Bio-Rad Laboratories, Inc., Melville, NY, USA) and Coomassie blue gel staining. Lysates were run on a 10% SDS-PAGE gel and transferred to a polyvinylidene difluoride (PVDF) membrane. After blocking, the membrane was probed with the following primary antibodies: Slug (G-18, Santa Cruz Biotechnology), PPAR-gamma (H-100 and E-8, Santa Cruz Biotechnology), RXRalpha (D-20, Santa Cruz Biotechnology), C/EBPbeta (C-19, Santa Cruz Biotechnology), C/EBPdelta (M-17, Santa Cruz Biotechnology), C/EBPalpha (14AA, Santa Cruz Biotechnology), FABP4 (aP2) (no. 10004944, Cayman Chemical), Glut4 (Cell Signalling, no. 2229), adiponectin (USBiological, A0890-05), adiponectin (Chemicon International, no. MAB3608) and actin (I-19, Santa Cruz Biotechnology). Reactive bands were detected with an enhanced chemiluminescence system (ECL) system (Amersham).

### Luciferase assays

The reporter containing the proximal part of the hPPAR $\gamma$ 2 promoter cloned in front of the luciferase gene (pGL3-hPPAR $\gamma$ 2p1000 vector) was kindly provided by Johan Auwerx (19). The ratC/EBP $\alpha$ wtpSG5 and ratC/EBP $\beta$ wtpSG5 expression vectors were kindly provided by Dr Achim Leutz (37). The expression vector pcDNA3-mSlug was generated by cloning the mouse Slug cDNA into the expression plasmid pcDNA3. For reporter assays, U2OS cells or Slug-deficient MEFs were transfected using Dual-Luciferase (Promega) with normalization to Renilla luciferase, and mean  $\pm$  standard error was determined from at least three data points. U2OS cells and Slug-deficient MEFs were maintained in DMEM supplemented with 10% FBS.

### Histone acetylation status

Surgical tissues removed from control, Combi-Slug and Slug-deficient mice were washed twice in ice-cold PBS supplemented with 5 mM sodium butyrate to retain levels of histone acetylation and homogenized in cold-TEB [PBS containing 0.5% Triton X-100 (v/v), 2 mM phenylmethylsulfonyl fluoride and 0.02% (v/v) Na $_3$ N], placed on ice for 10 min with gentle stirring, centrifuged and washed in cold TEB. Pellet was resuspended in 0.2N HCl and histones were extracted overnight at 4°C. Supernatant recovered acidic extraction was subjected to SDS-PAGE, transferred onto a PVDF 22  $\mu$ m pore size (Immobilon PSQ; Millipore) and immunoblotted with anti-acetylated histone H3 (Upstate Biotechnology, Lake Placid, NY, USA). Core histones loading control was performed with a classical Coomassie staining of acidic proteins extract. The signal was detected with ECL (Amersham Pharmacia Biotech, UK limited), according to the protocols recommended by the manufacturer.

### ChIP assay

Mouse tissues (WAT and liver) were removed surgically from different mice (*wt*, *Combi-SLUG* and *SLUG* $^{-/-}$ ), homogenized and disaggregated in 2 mg/ml of Collagenase (Sigma, Type I) ON at 37°C. Cells were fixed *in vivo* at room temperature for 15 min by the addition of crosslinking mix (11% formaldehyde; 100 mM NaCl; 0.5 mM EDTA; 50 mM HEPES, pH 8.0) at a final concentration of 1% directly onto the tissue disaggregating media. Fixation was quenched by addition of glycine with a 0.125 M final concentration and the incubation was continued for a further 5 min. The cells were washed twice using ice-cold PBS and collected. The cell pellets were washed and dissolved with cell lysis buffer [50 mM Tris-HCl (pH 8.0), 10 mM EDTA, pH 8.0; 1% SDS and a protease inhibitor cocktail (Roche)] and remained on ice for 10 min. The cell lysates were sonicated to shear chromosomal DNA with an average length of 500–1000 bp. After centrifugation to remove insoluble materials, the chromatin solution was diluted in a mixture of nine parts dilution buffer [1% Triton X-100; 150 mM NaCl; 2 mM EDTA, pH 8.0; 20 mM Tris-HCl, pH 8.0 and a protease inhibitor cocktail (Sigma)] 1 part lysis buffer, and the diluted solution was pre-cleared with protein G-Sepharose beads on a rotating wheel at 4°C for 1 h. Beads were removed by centrifugation and the supernatants were incubated with 2 mg of antibodies to HDAC (H-51), SLUG (H-140) and c/EBP $\alpha$  (14AA) from Santa Cruz Biotechnology Inc. (Santa Cruz, CA, USA) or acetylated histone H3 from Upstate Biotechnology at 4°C overnight. The complexes were immunoprecipitated with protein G-Sepharose beads 2 h at 4°C. The beads were washed once with IP dilution buffer, twice with wash buffer (20 mM Tris-HCl (pH 8.0), 150 mM NaCl, 2 mM EDTA, 1% Triton X-100, 0.1% SDS and a protease inhibitor cocktail), once with final wash buffer (20 mM Tris-HCl, pH 8.0, 500 mM NaCl, 2 mM EDTA, 1% Triton X-100, 0.1% SDS and a protease inhibitor cocktail) and twice with TE buffer. Immune complexes were eluted from the beads in the elution buffer (1% SDS; 100 mM NaHCO $_3$ ) for 15 min. The proteins were removed from DNA by digesting with proteinase K and RNase A (500  $\mu$ g/ml each) at 37°C for 1 h. The crosslink was reversed by adding 5 M NaCl to a final concentration of 200 mM, followed by incubation at 65°C for 6 h. The sample DNAs were then extracted with phenol-chloroform-isoamyl alcohol (25:24:1), precipitated with cold-ethanol and resuspended in TE buffer. Similarly, purified DNA fragments from the chromatin extracts (input) were used as a control for PCR reactions. Precipitated DNAs were analysed by PCR of 30 cycles using primers: m-PPAR $\gamma$ 2-ChIP-1F 5'-gtacagttcagccctcac-3'; m-PPAR $\gamma$ 2-ChIP-1R 5'-ttgggagaggtgggaa-3'; m-PPAR $\gamma$ 2-ChIP-2F 5'-caggaattattgccatctga-3' and m-PPAR $\gamma$ 2-ChIP-2R 5'-ggcaaggaattgtgtcagt-3'; m-PPAR $\gamma$ 2-ChIP-3F 5'-ctgttgaataacacctt-3'; m-PPAR $\gamma$ 2-ChIP-3R 5'-cagtggcttttaaatagaa-3'; covering 205, 212 and 219 bp, respectively, from PPAR $\gamma$ 2 promoter. PCR products were separated on a 2% agarose gel and stained with ethidium bromide.

### SUPPLEMENTARY MATERIAL

Supplementary Material is available at HMG Online.

## ACKNOWLEDGEMENTS

We thank the members of Lab 13 at IBMCC for advice and criticism and Manuel Sanchez-Martin for assistance with figures. We are grateful to Dr Tyler Jacks and Julian Sage for various useful reagents. We would like to thank Dave Tuveson for his support and helpful discussions, Dr Johan Auwerx for the pGL3-hPPAR $\gamma$ 2p1000 vector, Dr Achim Leutz for the ratC/EBP $\alpha$ wtpSG5 and ratC/EBP $\beta$ wtpSG5 expression vectors and Dr T. Gridley for the Slug mutant mice.

*Conflict of Interest statement.* None declared.

## FUNDING

The research is supported partially by FEDER and MEC (SAF2006-03726 and PETRI no. 95-0913.OP), Junta de Castilla y León (CSI03A05), FIS (PI050087, PI050116), Fundación de Investigación MMA, Federación de Cajas de Ahorro Castilla y León (I Convocatoria de Ayudas para Proyectos de Investigación Biosanitaria con Células Madre), CDTEAM project (CENIT-Ingenio 2010) and MEC Consolider-Ingenio 2010 (ref. CSD2007-0017).

## REFERENCES

- Morrison, R.F. and Farmer, S.R. (2000) Hormonal signaling and transcriptional control of adipocyte differentiation. *J. Nutr.*, **130**, 3116S–3121S.
- Rosen, E.D., Walkey, C.J., Puigserver, P. and Spiegelman, B.M. (2000) Transcriptional regulation of adipogenesis. *Genes Dev.*, **14**, 1293–1307.
- Soukas, A., Soccia, N.D., Saatkamp, B.D., Novelli, S. and Friedman, J.M. (2001) Distinct transcriptional profiles of adipogenesis *in vivo* and *in vitro*. *J. Biol. Chem.*, **276**, 34167–34174.
- Chen, Z., Torrens, J.I., Anand, A., Spiegelman, B.M. and Friedman, J.M. (2005) Krox20 stimulates adipogenesis via C/EBP $\beta$ -dependent and -independent mechanisms. *Cell Metab.*, **1**, 93–106.
- Sefton, M., Sanchez, S. and Nieto, M.A. (1998) Conserved and divergent roles for members of the Snail family of transcription factors in the chick and mouse embryo. *Development*, **125**, 3111–3121.
- Sanchez-Martin, M., Gonzalez-Herrero, I. and Sanchez-Garcia, I. (2004) SNAI2 (SNAIL HOMOLOG 2) Atlas Genet Cytogenet Oncol Haematol. <http://atlasgeneticsoncology.org/Genes/SNAI2ID453.html>. April.
- Inoue, A., Seidel, M.G., Wu, W., Kamizono, S., Ferrando, A.A., Bronson, R.T., Iwasaki, H., Akashi, K., Morimoto, A., Hitzler, J.K. *et al.* (2002) Slug, a highly conserved zinc finger transcriptional repressor, protects hematopoietic progenitor cells from radiation-induced apoptosis *in vivo*. *Cancer Cell*, **2**, 279–288.
- Perez-Losada, J., Sanchez-Martin, M., Rodriguez-Garcia, A., Sanchez, M.L., Orfao, A., Flores, T. and Sanchez-Garcia, I. (2002) Zinc-finger transcription factor Slug contributes to the function of the stem cell factor c-kit signaling pathway. *Blood*, **100**, 1274–1286.
- Perez-Losada, J., Sanchez-Martin, M., Perez-Caro, M., Perez-Mancera, P.A. and Sanchez-Garcia, I. (2003) The radioresistance biological function of the SCF/kit signaling pathway is mediated by the zinc-finger transcription factor Slug. *Oncogene*, **22**, 4205–4211.
- Pérez-Mancera, P.A., González-Herrero, I., Pérez-Caro, M., Gutiérrez-Cianca, N., Flores, T., Gutiérrez-Adán, A., Pintado, B., Sanchez-Martin, M. and Sanchez-Garcia, I. (2005) SLUG (SNAI2) in cancer development. *Oncogene*, **24**, 3073–3082.
- Cohen, M.E., Yin, M., Paznekas, W.A., Schertzer, M., Wood, S. and Jabs, E.W. (1998) Human SLUG gene organization, expression, and chromosome map location on 8q. *Genomics*, **51**, 468–471.
- Sanchez-Martin, M., Rodriguez-Garcia, A., Perez-Losada, J., Sagraera, A., Read, A.P. and Sanchez-Garcia, I. (2002) SLUG (SNAI2) deletions in patients with Waardenburg disease. *Hum. Mol. Genet.*, **11**, 3231–3236.
- Oram, K.F., Carver, E.A. and Gridley, T. (2003) Slug expression during organogenesis in mice. *Anat. Rec.*, **271A**, 189–191.
- Sanchez-Martin, M., Perez-Losada, J., Rodriguez-Garcia, A., Gonzalez-Sanchez, B., Korf, B.R., Kuster, W., Moss, C., Spritz, R.A. and Sanchez-Garcia, I. (2003) Deletion of the SLUG (SNAI2) gene results in human piebaldism. *Am. J. Med. Genet.*, **122A**, 125–132.
- Perez-Mancera, P.A., Gonzalez-Herrero, I., Maclean, K., Turner, A.M., Yip, M.Y., Sanchez-Martin, M., Garcia, J.L., Robledo, C., Flores, T., Gutierrez-Adan, A., Pintado, B. and Sanchez-Garcia, I. (2006) SLUG (SNAI2) overexpression in embryonic development. *Cytogenet. Genome Res.*, **114**, 24–29.
- Zhang, J., Fu, M., Cui, T., Xiong, C., Xu, K., Zhong, W., Xiao, Y., Floyd, D., Liang, J., Li, E., Song, Q. and Chen, Y.E. (2004) Selective disruption of PPAR $\gamma$  2 impairs the development of adipose tissue and insulin sensitivity. *Proc. Natl Acad. Sci. USA*, **101**, 10703–10708.
- Tontonoz, P., Hu, E. and Spiegelman, B.M. (1994) Stimulation of adipogenesis in fibroblasts by PPAR  $\gamma$  2, a lipid-activated transcription factor. *Cell*, **79**, 1147–1156.
- Wu, Z., Rosen, E.D., Brun, R., Hauser, S., Adelmant, G., Troy, A.E., McKeon, C., Darlington, G.J. and Spiegelman, B.M. (1999) Cross-regulation of C/EBP  $\alpha$  and PPAR  $\gamma$  controls the transcriptional pathway of adipogenesis and insulin sensitivity. *Mol. Cell.*, **3**, 151–158.
- Fajas, L., Auboeuf, D., Raspe, E., Schoonjans, K., Lefebvre, A.M., Saladin, R., Najib, J., Laville, M., Fruchart, J.C., Deeb, S. *et al.* (1997) The organization, promoter analysis, and expression of the human PPAR $\gamma$  gene. *J. Biol. Chem.*, **272**, 18779–18789.
- Peinado, H., Ballestar, E., Esteller, M. and Cano, A. (2004) Snail mediates E-cadherin repression by the recruitment of the Sin3A/histone deacetylase 1 (HDAC1)/HDAC2 complex. *Mol. Cell. Biol.*, **24**, 306–319.
- Bermejo-Rodríguez, C., Pérez-Caro, M., Pérez-Mancera, P.A., Sánchez-Beato, M., Piris, M.A. and Sánchez-García, I. (2006) Mouse cDNA microarray analysis uncovers SLUG targets in mouse embryonic fibroblasts. *Genomics*, **87**, 113–118.
- Ayer, D.E. (1999) Histone deacetylases: transcriptional repression with SINers and NuRDs. *Trends Cell. Biol.*, **19**, 193–198.
- Cao, Z., Umek, R.M. and McKnight, S.L. (1991) Regulated expression of three C/EBP isoforms during adipose conversion of 3T3-L1 cells. *Genes Dev.*, **5**, 1538–1552.
- Lin, F.T. and Lane, M.D. (1994) CCAAT/enhancer binding protein  $\alpha$  is sufficient to initiate the 3T3-L1 adipocyte differentiation program. *Proc. Natl Acad. Sci. USA*, **91**, 8757–8761.
- Rosen, E.D., Hsu, C.H., Wang, X., Sakai, S., Freeman, M.W., Gonzalez, F.J. and Spiegelman, B.M. (2002) C/EBP $\alpha$  induces adipogenesis through PPAR $\gamma$ : a unified pathway. *Genes Dev.*, **16**, 22–26.
- Marks, P.A. and Jiang, X. (2005) Histone deacetylase inhibitors in programmed cell death and cancer therapy. *Cell Cycle*, **4**, 549–551.
- Yoo, E.J., Chung, J.J., Choe, S.S., Kim, K.H. and Kim, J.B. (2006) Down-regulation of histone deacetylases stimulates adipocyte differentiation. *J. Biol. Chem.*, **281**, 6608–6615.
- Inukai, T., Inoue, A., Kurosawa, H., Goi, K., Shinjyo, T., Ozawa, K., Mao, M., Inaba, T. and Look, A.T. (1999) SLUG, a ces-1-related zinc finger transcription factor gene with antiapoptotic activity, is a downstream target of the E2A-HLF oncoprotein. *Mol. Cell*, **4**, 343–352.
- Khan, J., Bittner, M.L., Saal, L.H., Teichmann, V., Azorsa, D.O., Gooden, G.C., Pavan, W.J., Trent, J.M. and Meltzer, P.S. (1999) cDNA microarrays detect activation of a myogenic transcription program by the PAX3–FKHR fusion gene. *Proc. Natl Acad. Sci. USA*, **96**, 13264–13269.
- Wasserman, F. (1965) The development of adipose tissue. In Renold, A. and Cahill, G. (eds), *Handbook of Physiology*, Vol. **Vol. 5**, American Physiological Society, Washington, DC, pp. 87–100.
- Cinti, S. (2000) Anatomy of the adipose organ. *Eat. Weight Disord.*, **5**, 132–142.
- Cobaleda, C., Perez-Caro, M., Vicente-Dueñas, C. and Sanchez-Garcia, I. (2007) Function of zinc-finger transcription factor SNAI2 in cancer and development. *Annu. Rev. Genet.*, Epub ahead of print June 5, 2007.
- Aybar, M.J., Nieto, M.A. and Mayor, R. (2003) Snail precedes slug in the genetic cascade required for the specification and migration of the *Xenopus* neural crest. *Development*, **130**, 483–494.
- Bolos, V., Peinado, H., Perez-Moreno, M.A., Fraga, M.F., Esteller, M. and Cano, A. (2003) The transcription factor Slug represses E-cadherin expression and induces epithelial to mesenchymal transitions: a comparison with Snail and E47 repressors. *J. Cell. Sci.*, **116**, 499–511.

35. Jiang, R., Lan, Y., Norton, C.R., Sundberg, J.P. and Gridley, T. (1998) The Slug gene is not essential for mesoderm or neural crest development in mice. *Dev. Biol.*, **198**, 277–285.
36. Castellanos, A., Pintado, B., Wuruaga, E., Arévalo, R., López, A., Orfao, A. and Sánchez-García, I. (1997) A BCR-ABL(p190) fusion gene made by homologous recombination causes B-cell acute lymphoblastic leukemias in chimeric mice with independence of the endogenous bcr product. *Blood*, **90**, 2168–2174.
37. Calkhoven, C.F., Muller, C. and Leutz, A. (2000) Translational control of C/EBPalpha and C/EBPbeta isoform expression. *Genes Dev.*, **14**, 1920–1932.